Applied Thermal Engineering 244 (2024) 122734

Contents lists available at ScienceDirect

Applied Thermal Engineering

journal homepage: www.elsevier.com/locate/ate

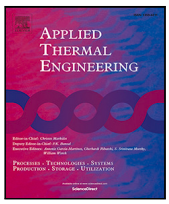

Research Paper

Chemical Reactor Network modeling of ammonia–hydrogen combustion in a gas turbine: stochastic sensitivity analysis

Rachele Lamioni *, Alessandro Mariotti, Maria Vittoria Salvetti, Chiara Galletti

Dipartimento di Ingegneria Civile e Industriale, Università di Pisa, 56122 Pisa, Italy

ARTICLE INFO

Keywords:
Hydrogen
CRN
Gas turbine
Ammonia
Decarbonization
NOx emissions

ABSTRACT

To tackle climate change, we need to incorporate renewable energy sources on a large scale. One potential solution is the use of hydrogen, as an alternative energy vector that can be burnt in existing devices with little modification. Hydrogen can be produced from excess wind and solar power, ammonia, as a hydrogen carrier, is very appealing as it can be easily liquefied and distributed through the existing infrastructure. This study aims to explore the feasibility of using ammonia–hydrogen mixtures in industrial settings. This exploration is made by modeling a gas turbine system through a network of chemical reactors (CRN) and it is aimed at improving our understanding of the energy conversion process involving hydrogen, ammonia, and their mixtures. In this work, we analyze the most significant parameters of the CRN model, leveraging stochastic techniques. Specifically, we study the effects of the model and operational parameters on NOx emissions. This could represent a valuable aid in the development of CRN models capable of predicting emissions from gas turbine systems, to understand the impact of various operating conditions, such as pressure, temperature, equivalence ratio, and mixture composition.

1. Introduction

Nowadays, ammonia NH_3 is attracting increasing attention for the decarbonization of power generation in gas turbines. Indeed, ammonia can act as a carrier of green hydrogen, as ammonia is easier to store and transport than hydrogen. This is made possible by the existing infrastructure, which is already well-established due to the extensive use of ammonia in agriculture. However, the main drawbacks associated with ammonia combustion are its low reactivity and significant nitrogen oxide (NOx) emissions compared to conventional hydrocarbon fuels. In particular, the laminar flame velocity for a NH_3/air-premixed flame is considerably low, around 7 cm/s, while the calorific value of ammonia is 18.6 MJ/kg. Therefore, the development of strategies to increase the combustion rate is imperative for the practical application of ammonia combustion. Several fundamental investigations on ammonia combustion have been carried out to address this challenge. Many ammonia gas turbine combustors employ highly directional flow, as observed in studies by Pugh et al. [1] and Valera-Medina et al. [2], resulting in the creation of significant recirculation zones within the combustor. These recirculation zones facilitate the reaction of unburned mixtures by transporting heat and radicals and by reducing the local flow velocity. Enhancing turbulent mixing can increase the turbulent flame velocity above the laminar flame velocity and contribute to flame stabilization, as highlighted in Wang et al. [3]. In addition, blending ammonia with more reactive fuels such as methane [4] or hydrogen [5,6], also obtained from ammonia cracking [7], is another strategy to improve the combustion process. One of the primary challenges in devising systems that can effectively exploit the potential of NH_3, H_2, and their mixtures is due to the complex chemical reactions and their interplay with other physical phenomena occurring within the combustion chamber. Indeed, the reaction kinetics, species transport and mixing, and heat transfer are influenced by numerous factors, including the composition of the fuel mixture, temperature, pressure, and flow conditions. As a result, accurately predicting emissions, particularly NOx, is a challenging task. In this context, numerical models and simulations can serve as valuable tools to assist and guide the design of new combustion systems able to efficiently dealing with these novel fuels. On the other hand, the use of computational fluid dynamics (CFD) techniques requires high computational costs due to the need to include detailed chemistry for reliable estimations of emissions, such as NOx and CO. Consequently, modeling techniques with lower computational costs have been developed, such as Chemical Reactor Networks (CRNs). This methodology, originally introduced by Bragg [8], offers a cost-effective approach for providing a simplified representation of complex thermochemical and flow fields. This is achieved by dividing the domain into a limited number of discrete volumes which are modeled as canonical chemical reactors,

* Corresponding author.
E-mail address: rachele.lamioni@unipi.it (R. Lamioni).

https://doi.org/10.1016/j.applthermaleng.2024.122734
Received 11 September 2023; Received in revised form 20 December 2023; Accepted 13 February 2024
Available online 15 February 2024

typically Perfectly Stirred Reactors (PSRs) and/or Plug Flow Reactors (PFRs). These interconnected reactors exchange mass and heat, creating a network designed to retain the essential characteristics of the entire flow field. Consequently, devising an equivalent CRN model for a specific system is not a straightforward task, as the model's effectiveness is significantly influenced by the chosen network configuration. The structure of this network can be predetermined based on flow considerations, as recommended by Andreini and Facchini [9] and, then, used for parametric emission studies on typical gas turbine combustors. CRN can also be used, as in Yousefian et al. [10,11], for quantifying uncertainty in lean premixed combustion across various operational conditions. Low-cost computational techniques have emerged, yielding promising outcomes. In several studies [12–19], CRNs have been meticulously designed, taking specific use from CFD simulation results. These investigations involve the identification of pertinent regions within the combustor, typically based on temperature and velocity fields. Other works have introduced a more systematic approach through zonal division, grouping computational CFD cells according to local temperature and stoichiometry [20–27]. However, these approaches often entail a substantial number of reactors (around $\simeq 102$), resulting in computationally intensive simulations. Utilizing a smaller number of reactors can enable the development of a tool capable of providing real-time predictions, as exemplified by Kaluri et al. [28], who achieved real-time lean-blowout prediction. In the same test case, a CRN-based control system is devised to prevent lean-blowout [29]. Recently, Chaturvedi et al. [30] studied the NOx emissions from a 70%NH_3–30%H_2 (by. vol) premixed combustion using a CRN approach based on CFD simulations. The research included a comparison of experimental NO emission and those predicted with different kinetic mechanisms. The authors found that the stoichiometry, i.e., the air excess, controls formation pathways and thus emissions. The results provide a good understanding of the intricate processes influencing NOx emissions in NH_3–H_2 combustion.

The present study adopts a simple one-stage CRN model to predict the emissions of NH_3–H_2 combustion within gas turbines for a comprehensive range of operational conditions and model parameters. In particular, we consider a high-pressure swirl burner (HPGSB-2) fueled with an NH_3–H_2 mixture [1,2]. The objective of this work is indeed to characterize the effect of model and operational parameters on the estimation of NOx emissions. In particular, stochastic techniques are employed to obtain a fast and detailed description of the response of NOx emissions to changes in the considered parameters starting from a limited number of numerical simulations. This kind of information pivotal in fine-tuning the combustion process and emissions management. The final aim is to set-up a methodological approach, which could through a methodical inquiry, bolster our capacity to forecast and mitigate emissions, ultimately fostering the development of more efficient and sustainable gas turbine systems propelled by NH_3–H_2 blends.

2. Chemical reactor network

The present CRN model is developed using the open-source software CANTERA [31], interfaced with Python, to emulate the Swirled High-Pressure Vortex Combustor (HPGSB-2) developed at the Gas Turbine Research Center of Cardiff University [1,32]. The combustor is characterized by a premixed feed, with the option of introducing a secondary air injection to enable the use of fuel-rich primary mixtures. The CRN is applied to the one-stage configuration (i.e. without secondary air injection). The network configuration consists of two Perfectly Stirred Reactors (PSRs) to represent the mixing zone, where no reaction occurs, and the recirculating premixed flame zone, where injection through an H_2 radicals reservoir is applied for ignition. Subsequently, a Plug Flow Reactor (PFR) is used to mimic the post-flame zone. The scheme of the network is reported in Fig. 1. In particular, the PFR is modeled using a series of PSR reactors. The number of chosen reactors, i.e., 2000, is estimated through a preliminary analysis that demonstrated the independence of the results with a further increase in this number.

2.1. CRN validation

For validation purposes, the 70%NH_3 and 30%H_2 test case by Pugh et al. [1] is taken as the reference. The fresh mixture temperature and pressure are $T = 423$ K and $p = 0.105$ MPa respectively. The volume of the reactive PSR is estimated based on a residence time of 5 ms in agreement with the work by Alnasif et al. [33]. In the simulations, an adiabatic condition is assumed, i.e., the reactors do not exchange heat with the environment.

The following kinetic mechanisms are compared:

- Stagni et al. [34] with 31 species and 203 reversible reactions;
- Gotama et al. [35] with 32 species and 165 reversible reactions;
- Okafor et al. [4] with 59 species and 256 reversible reactions.
- Otomo et al. [36] with 32 species and 213 reversible reactions.

Fig. 2 compares the predicted NOx emissions, normalized with respect to 15% O_2 in the flue gases, to experimental data [1]. We can notice that all chosen kinetic mechanisms capture the overall trend of NOx emissions. However, the best fit with experimental data is achieved with the Okaor et al. and Gotama et al. kinetic mechanisms. For the subsequent analyses, Gotama et al. is chosen as a good compromise between computational cost and reliability in predicting emissions for NH_3–H_2 mixtures. To further validate the Gotama et al. mechanism, Fig. 2 also compares its prediction of the unburned ammonia to the experimental data, again showing an encouraging agreement.

3. Uncertainty quantification

A stochastic sensitivity analysis is conducted using the Generalized Polynomial Chaos (gPC) method, to investigate the impact of operational and model parameters on the estimation of NOx emissions within the CRN model. More specifically, the Polynomial Chaos Expansion (PCE) and sensitivity analysis are performed using an in-house tool developed within the Dakota open-source code. The goal is to generate continuous response surfaces of the quantities of interest within the parameter space while minimizing the number of simulations and ensuring a high level of result accuracy.

In the generalized polynomial chaos method, a quantity of interest, Z, is written through the following polynomial expansion [37]:

$$Z(\epsilon) = \sum_{j=0}^{\infty} b_j \Psi_j(\boldsymbol{\zeta}(\epsilon)) \tag{1}$$

where $\boldsymbol{\zeta}$ is the vector of the uncertain independent parameters, ϵ is an aleatory event, $\Psi_j(\boldsymbol{\zeta})$ is the jth gPC polynomial and b_j is the corresponding projection coefficient.

The response surface of the considered quantity is computed by truncating the expansion in Eq. (1) to the limit O, which can be calculated as follows:

$$O = \prod_{k=1}^{N} (T_k + 1) - 1 \tag{2}$$

where N is the dimension of the $\boldsymbol{\zeta}$-vector, the index k identifies the particular random variable within that vector, and T_k is the maximum order of the corresponding polynomial.

Finally, the coefficient b_j is defined as follows:

$$b_j = \frac{\langle Z, \Psi_j \rangle}{\langle \Psi_j, \Psi_j \rangle} = \frac{1}{\langle \Psi_j, \Psi_j \rangle} \int_{\text{supp}\,\boldsymbol{\zeta}} Z \Psi_j \omega(\boldsymbol{\zeta}) \mathrm{d}\boldsymbol{\zeta} \tag{3}$$

where $\omega(\boldsymbol{\zeta})$ is the weight function connected to Ψ_j. In this paper, the integral in Eq. (3) is numerically computed by using a Gaussian quadrature formula. The polynomial family Ψ_j has to be *a priori* defined and a suitable choice accelerates the convergence of the procedure. For the Gaussian quadrature, the optimal family is the one having a weight function analogous to the probability measure of the input random

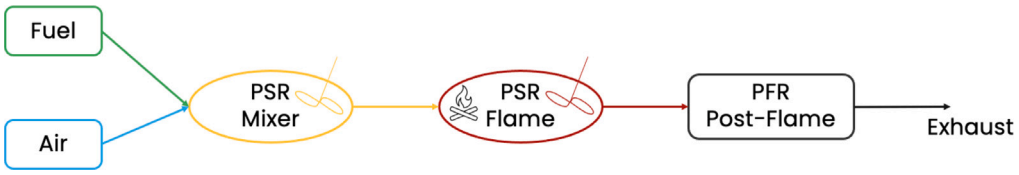

Fig. 1. Sketch of the one-stage CRN.

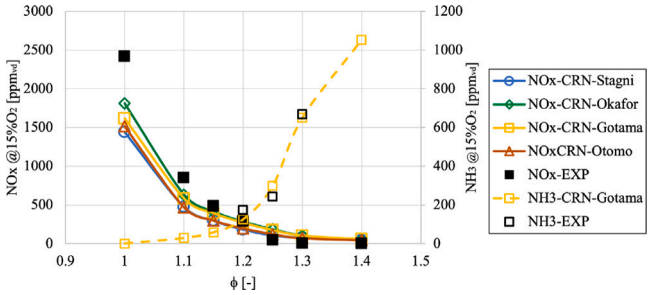

Fig. 2. NOx emissions normalized to 15% O_2 and unburnt NH_3 in the flue gases estimated with CRN model with respect to the equivalence ratio for different kinetic mechanisms compared with experimental data [1]. Mixture: 70%NH_3–30%H_2, $T = 423$ K and $p = 0.105$ MPa.

parameters. The selected polynomial family thus is related to the shape of the PDF of the uncertain parameters.

The total variance of the output quantities is:

$$V = \sum_{j=1}^{N} (b_j^*)^2 \tag{4}$$

with $b_j^* = b_j |\Psi_j|$, $|\Psi_j|$ being the norm of the jth polynomial.

The partial sensitivity to one of the parameters or to a combination of them is computed through the variance decomposition method [38]. Thus, the Sobol indexes (also called sensitivity indexes) I_i are evaluated as the ratios between the partial variance V_i due to the ith parameter, and V:

$$I_i = \frac{V_i}{V} \tag{5}$$

In this context, an analysis is carried out by varying four parameters. Three of them are related to the operating conditions, i.e.: the H_2 content in the NH_3–H_2 mixture, the equivalence ratio, and the fresh mixture inlet temperature (T_{in}). The fourth parameter concerns the modeling of the chemical reactor network and is represented by the volume fraction dedicated to the flame zone (PSR-flame) compared to the total volume of the combustion chamber (V_{PSR}/V_{tot}). The output variables, to analyze the effect of these parameters, are constituted by the NOx emissions (calculated taking into account the chemical species NO and NO_2) and the amount of unburned NH_3, recorded together with NOx at the outlet of the PFR reactor. In addition, the effect of these four parameters on the temperatures in both the PSR and PFR reactors is evaluated.

For the analysis, the ranges are set as follows: $\%H_2 \in [20\%, 80\%]$, $\phi \in [0.31, 1.4]$, and $V_{PSR} \in [10\%, 90\%]$ and $T_{in} \in [430\,\mathrm{K}, 700\,\mathrm{K}]$. As for $\%H_2$, the interval encompasses a wide range of variation, only excluding values very close to pure hydrogen or ammonia. The same is for V_{PSR}/V_{tot}, excluding values leading to a single reactor configuration. The variation interval of the equivalence ratio, ϕ, is chosen to avoid conditions at which combustion is not sustained. Finally, the range of variation of T_{in} is chosen taking into account realistic operational conditions. In these ranges, the uncertain-parameter PDF is considered to be uniform due to the lack of information on the distribution functions. This choice is also motivated by the fact that, among the classically used distributions, it is the least informative distribution with the highest variance in given intervals. The polynomials in Eq. (1) are, thus, Legendre polynomials.

We truncate the gPC expansion to the 3rd order in each dimension. Consequently, 4 quadrature points are considered for each parameter (Gauss–Legendre points). The Quadrature Points (QP) are summarized in Table 1. These are the parameter values for which numerical simulations have to be performed. Following a tensor product expansion, 256 simulations are carried out to evaluate the stochastic response surfaces for the emissions in terms of NOx, unburned NH_3 and reactor temperature. To analyze the effect of the kinetic scheme, we compare the stochastic response surfaces for NOx emissions using two different kinetic mechanisms, i.e. Stagni et al. and Gotama et al. schemes.

Table 1
Deterministic values considered for the analysis: equivalence ratio, H_2 content, volume of the PSR with respect to the total volume and temperature of the mixture.

QP	1st	2nd	3rd	4th
ϕ [−]	0.39	0.67	1.04	1.32
H_2 [%]	24.9	43.1	66.9	85.1
V_{PSR}/V_{tot} [%]	15	33	57	75
T_{in} [K]	449	519	611	681

4. Results

4.1. Effect of H_2 content, equivalence ratio, volume of the reacting PSR and inlet temperature

The sensitivity analysis involves varying the H_2 content in the NH_3-NH_3 mixture, the equivalence ratio (ϕ), the fraction of the total volume occupied by the reactor representing the reaction zone (V_{PSR}/V_{tot}), and the inlet temperature of the mixture T_{in} to assess the impact on NOx emissions, unburned NH_3 content, and reactor temperatures. Throughout this analysis, the injection pressure is maintained constant at $p = 1$ atm, while the kinetic mechanism is Gotama et al. based on the results of the CRN validation.

To visualize the quantities of interest, such as NOx emissions or unburned ammonia, we consider *slices* within the fourth-dimensional parameter space, fixing two parameters at a time. Fig. 3 presents NOx emissions, normalized to 15% O_2 in the flue gases as a color map in the H_2 - ϕ space for slices with fixed V_{PSR}/V_{tot} and inlet temperature T_{in} = 430 K, i.e., V_{PSR}/V_{tot} = 20% (Fig. 3a) and V_{PSR}/V_{tot} = 60% (Fig. 3b). The white markers indicate quadrature points where the numerical simulations through the CRN are carried out.

We observe that NOx emissions present maximum values for low equivalence ratio ($0.4 < \phi < 0.8$), while they decrease as the equivalence ratio increases. For equivalence ratios $\phi > 1.0$, NOx values decrease to less than 100 ppmv. On the other hand, for $0.4 < \phi < 0.8$ the NOx emissions range between 2000 and 5000 ppmv. In particular, increasing the PSR volume (V_{PSR}/V_{tot}) the NOx emissions decrease from the range 3000–5000 ppmvd to 2000–4000 ppmvd (Fig. 3a–b), while increasing the inlet mixture temperature T_{in} (at the same V_{PSR}/V_{tot}) leads to an increase of the NOx emissions to 6000 ppmvd (Fig. 3a–c). Despite the differences in NOx ranges, we observe that the zone with largest NOx emissions remains consistent, regardless of variations in the PSR volume or mixture inlet temperature.

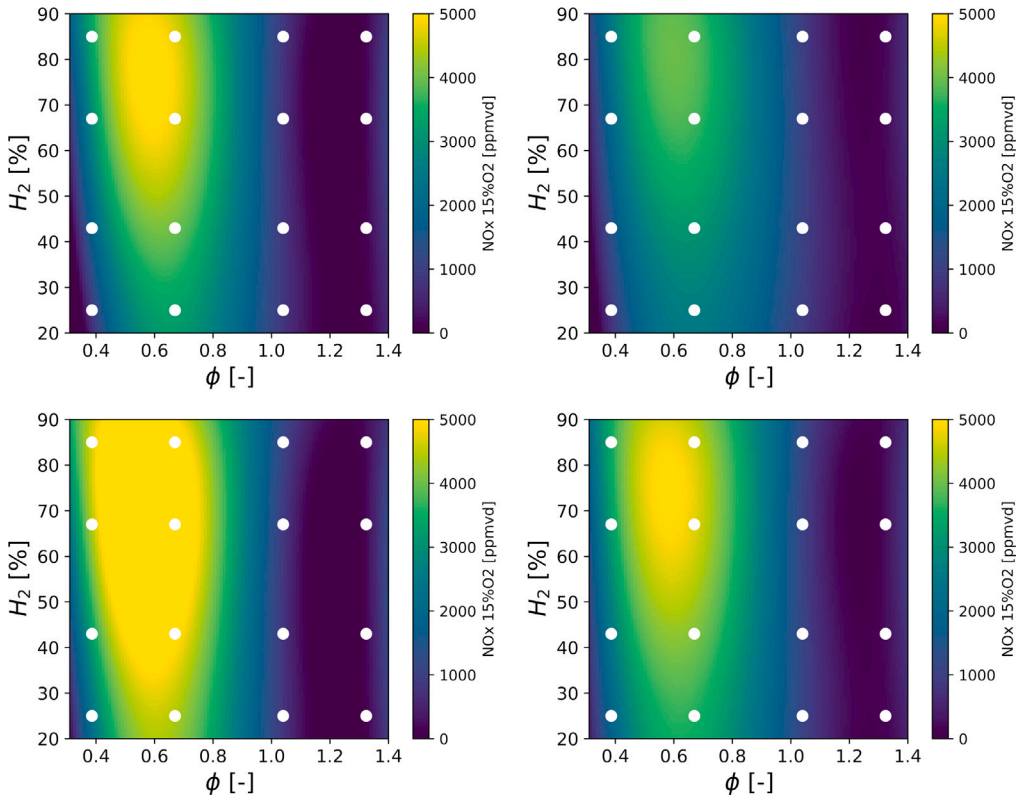

Fig. 3. Stochastic response surface of NOx emissions normalized to 15% O_2 in the flue gases in the parameter space of $\%H_2$ and ϕ with fixed reactor volume and inlet temperature. (a) $V_{PSR}/V_{tot} = 20\%$, $T_{in} = 430$ K, (b) $V_{PSR}/V_{tot} = 60\%$, $T_{in} = 430$ K, (c) $V_{PSR}/V_{tot} = 20\%$, $T_{in} = 600$ K, (d) $V_{PSR}/V_{tot} = 60\%$, $T_{in} = 600$ K. The white markers indicate quadrature points.

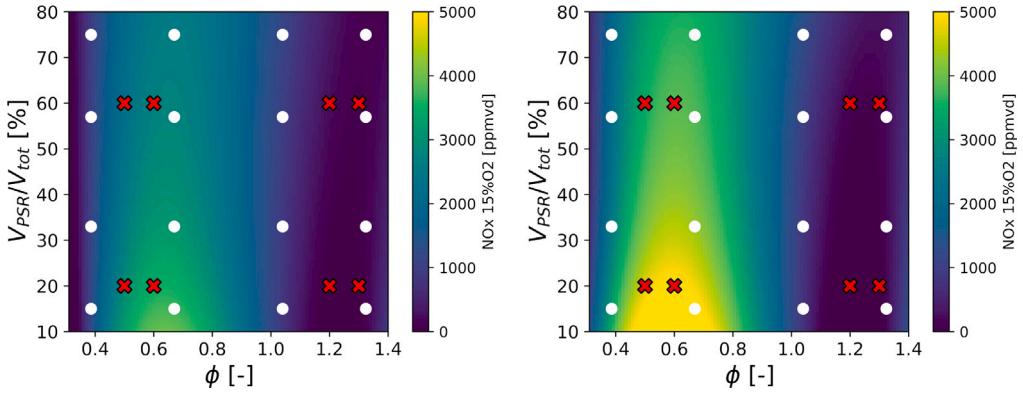

Fig. 4. Stochastic response surface of NOx emissions normalized to 15% O_2 in the flue gases, in the parameter space of ϕ and $\%V_{PSR}/V_{tot}$ with fixed H_2 content and inlet temperature $T_{in} = 430$ K. (a) $\%H_2 = 30\%$, (b) $\%H_2 = 70\%$. The white markers indicate quadrature points and the red crosses indicate test points.

To investigate the effect of the volume of the reacting PSR on NOx emissions, we present their stochastic response surface (in a slice) in ϕ-V_{PSR}/V_{tot} space, fixing the H_2 content to $\%H_2 = 30\%$ in Fig. 4a and $\%H_2 = 70\%$ in Fig. 4b. Once again, we observe that NOx emissions are strongly dependent on the equivalence ratio, while they are not appreciably affected by the PSR volume. The NOx values do not exhibit significant differences when maintaining a constant equivalence ratio, except for an area between $\phi = 0.5$ and 0.6, and $V_{PSR}/V_{tot} = 20\%$–30%, where the maximum values of NOx emissions are recorded. After obtaining the response surface, additional eight simulations are performed for the $70\%NH_3$–$30\%H_2$ mixture, maintaining an inlet temperature of $T_{in} = 430$ K and varying $\phi = 0.4, 0.5, 1.2$ and 1.3, and $V_{PSR}/V_{tot} = 20\%$ and 60%. We can observe that the NOx emissions are found to be consistent with the response surface values at these points, with an error of less than 6%.

In the same parameter space, Fig. 5 presents the unburned ammonia obtained for a fixed $V_{PSR}/V_{tot} = 20\%$ (Fig. 5a) and $V_{PSR}/V_{tot} = 60\%$ (Fig. 5b). We can note that the decrease of NOx emissions with the equivalence ratio is accompanied by the undesirable increase of unburned NH_3. This effect could be mitigated by devising a secondary air injection [39,40].

Fig. 6 shows NOx emissions, normalized to 15% O_2 in the flue gases as a color map in the T_{in} - ϕ space for slices with fixed H_2 content $\%H_2 = 30\%$ and PSR reactor volume i.e., $V_{PSR}/V_{tot} = 20\%$ (Fig. 6a) and $V_{PSR}/V_{tot} = 60\%$ (Fig. 6b). We can note that the maps present a similar trend for different V_{PSR}/V_{tot} values.

To gain a better insight into the role of the different parameters, the Sobol's indices are reported in Fig. 7a and Fig. 7b for the NOx emissions and the unburned NH_3, respectively. The indices confirm that the dominant input parameter influencing NOx emissions is the equivalence ratio (ϕ), with a Sobol index of $I_\phi = 89.2\%$. All other

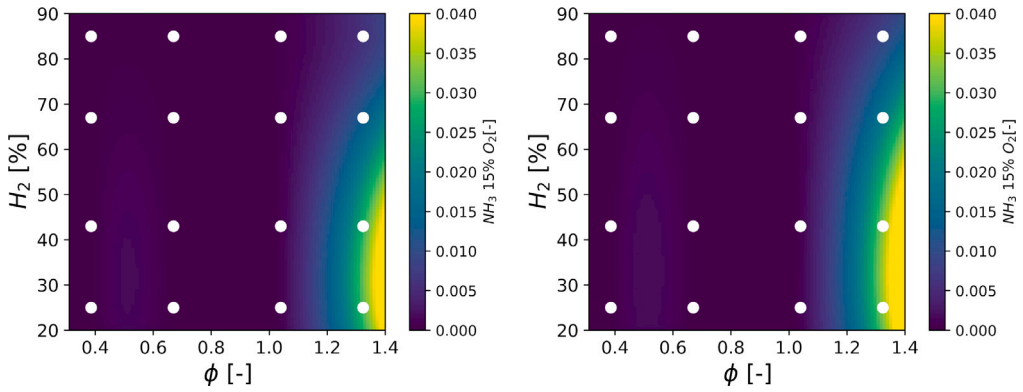

Fig. 5. Stochastic response surface of unburned NH_3 in the parameter space of $\%H_2$ and ϕ with fixed reactor volume and inlet temperature $T_{in} = 430$ K. (a) $V_{PSR}/V_{tot} = 20\%$, (b) $V_{PSR}/V_{tot} = 60\%$. The white markers indicate quadrature points.

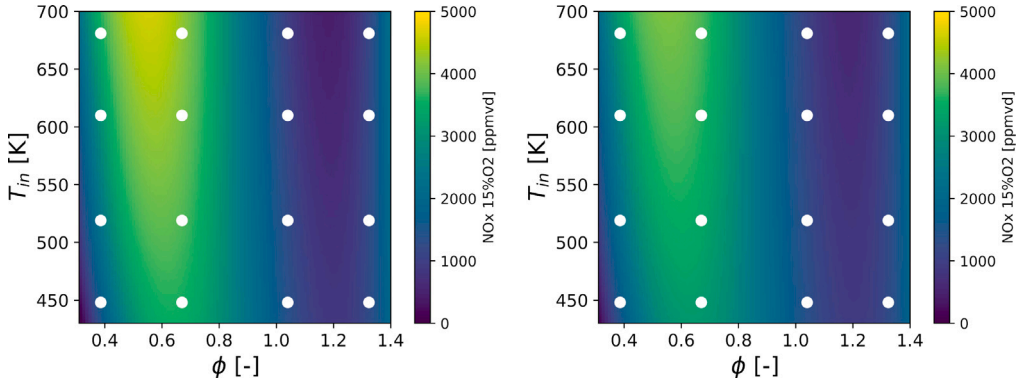

Fig. 6. Stochastic response surface of NOx emissions normalized to 15% O_2 in the flue gases, in the parameter space of ϕ and T_{in} with fixed H_2 content $\%H_2 = 30\%$ and reactor volume, (a) $V_{PSR}/V_{tot} = 20\%$, (b) $V_{PSR}/V_{tot} = 60\%$. The white markers indicate quadrature points.

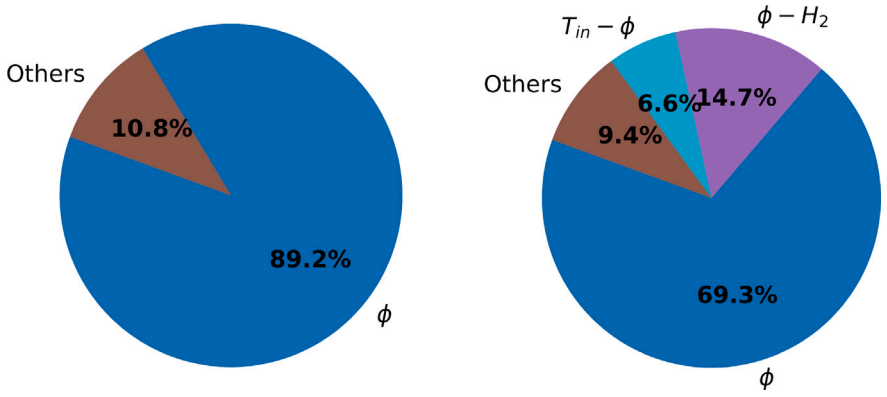

Fig. 7. Sobol' indices for corrected NOx emissions (a) and unburned NH_3 (b).

Sobol's indices, namely I_{H_2}, $I_{V_{PSR}/V_{tot}}$, $I_{T_{in}}$ and those identifying the coupled sensitivity to the parameters, i.e., $I_{T_{in},V_{PSR}/V_{tot}}$, $I_{\phi,V_{PSR}/V_{tot}}$, $I_{\phi,T_{in}}$, $I_{H_2,T_{in}}$, $I_{H_2,V_{PSR}/V_{tot}}$, I_{ϕ,H_2}, $I_{T_{in},\phi,V_{PSR}/V_{tot}}$, $I_{T_{in},H_2,V_{PSR}/V_{tot}}$, I_{T_{in},ϕ,H_2}, $I_{H_2,\phi,V_{PSR}/V_{tot}}$ and $I_{\phi,H_2,V_{PSR}/V_{tot},T_{in}}$, have negligible values, indicating their minimal influence on NOx emissions each index has a value less than 5%. Regarding the unburned NH_3 (Fig. 7b), the dominant parameter is the equivalence ratio (ϕ) with a Sobol index of $I_\phi = 69.3\%$, consistent with the fact that unburned NH_3 is a result of a fuel-rich condition There is also a weaker but still significant dependence on the Sobol interaction between the equivalence ratio and the hydrogen content, i.e. $I_{\phi,H_2} = 14.7\%$.

Finally, Fig. 8 shows temperature maps in the two reactors characterizing the CRN: the PSR (Fig. 8a) and the PFR (Fig. 8b), with a fixed reactor volume $V_{PSR}/V_{tot} = 20\%$ and a constant inlet temperature of $T_{in} = 430$ K. The stochastic response surface exhibits a strong dependence on the equivalence ratio ϕ with respect to the mixture composition ($\%H_2$). We observe that with a high H_2 content in the mixture and an equivalence ratio (ϕ) in the range between 1.0 and 1.2, there is an area with higher temperatures. This aligns with the

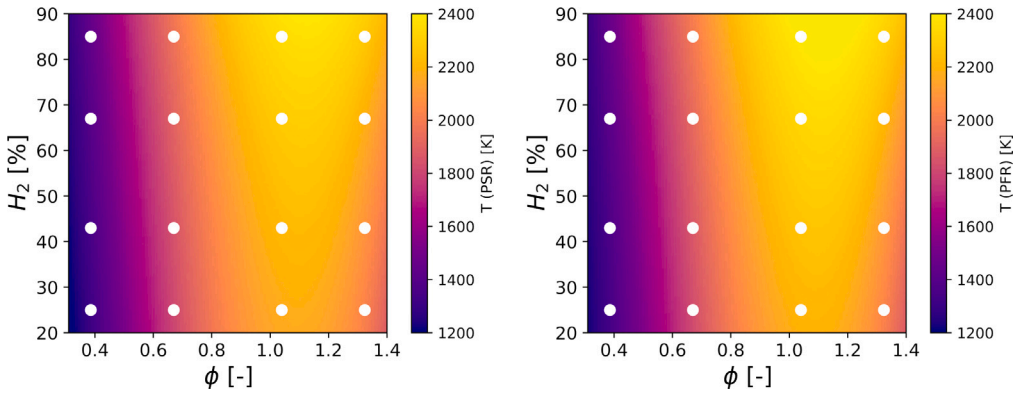

Fig. 8. Stochastic response surface of the temperature in the CRN PSR (a) and PFR (b) in the parameter space of $\%H_2$ and ϕ with fixed reactor volume $V_{PSR}/V_{tot} = 20\%$ and inlet temperature $T_{in} = 430$ K.

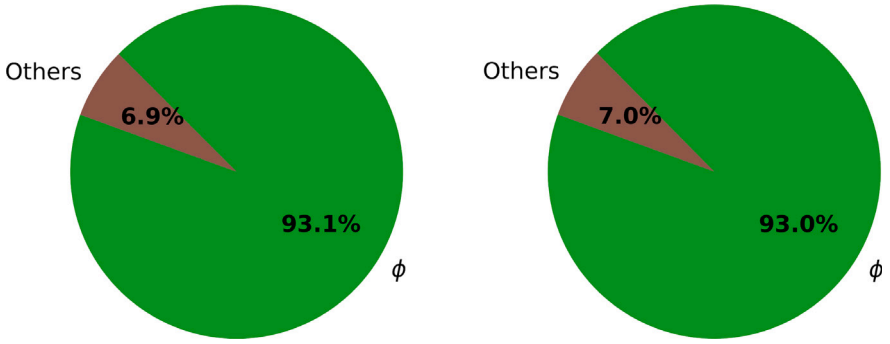

Fig. 9. Sobol' indices for temperature in PSR (a) and PFR (b) reactors.

fact that hydrogen exhibits the adiabatic temperature peak slightly to the right (i.e., richer conditions) compared to stoichiometric conditions ($\phi = 1.0$). This significant dependence on the equivalence ratio, in comparison to other parameters, is further confirmed by the Sobol indices illustrated in Fig. 9 for both PSR temperature (Fig. 9a) and PFR temperature (Fig. 9b). Notably, for both temperatures, the Sobol index associated with the equivalence ratio surpasses 90%, while the other indices hold negligible values.

4.2. Effect of the kinetic mechanism on NOx emissions

Fig. 10 illustrates the stochastic response surface of NOx in % H_2-ϕ space, with a fixed reactor volume of $V_{PSR}/V_{tot} = 20\%$ and an inlet temperature of $T_{in} = 430$ K. The analysis considers two kinetic mechanisms: Gotama et al. (Fig. 10a) and Stagni et al. (Fig. 10b), aiming to investigate their impact on NOx estimations. We can note that the maps exhibit a similar trend with different quantitative values of NOx emissions. In agreement with the results discussed in the CRN validation, the Stagni et al. mechanism underestimates the NOx emission with respect to the Gotama et al. scheme.

Fig. 11 shows the stochastic Probability Density Functions (PDFs) of NOx emissions using two kinetic mechanisms, i.e., Stagni et al. and Gotama et al. The PDFs exhibit two peaks: one around zero, representing areas of the response surfaces shown across the maps for $\phi > 0.8$, and the second peak representing the zone for equivalence ratios $0.4 < \phi < 0.8$. Upon comparing the two mechanisms through the PDFs, we observe that Stagni et al. has the second peak at lower NOx values compared to Gotama et al. again in accordance with the findings in the validation section.

5. Conclusions

In this study, a Chemical Reactor Network (CRN) is developed and implemented to emulate a gas turbine system fueled by a mixture of ammonia and hydrogen. The CRN is constructed using two PSR reactors, characterizing the mixing and reaction zones, and a PFR reactor emulating the post-combustion zone. The network is preliminary validated against experimental data. Subsequently, stochastic techniques employing gPC are applied to gain an in-depth understanding of the network model and operational parameters influencing NOx emissions and unburned NH_3. In particular, we consider three operational parameters, i.e., the H_2 content, the inlet temperature of the mixture T_{in} and the equivalence ratio ϕ, and a model parameter, i.e. the volume of the reacting PSR, i.e., V_{PSR}/V_{tot}.

An analysis is conducted by varying all four chosen parameters, % H_2-ϕ-V_{PSR}/V_{tot}-T_{in}, to assess their joint effect on the estimation of NOx emissions. We observe that NOx emissions are not significantly influenced by the volume of the PSR and the inlet temperature; however, they exhibit a strong dependence on the equivalence ratio, as further supported by the analysis of Sobol indices. We observe that we need to operate under rich conditions ($\phi > 1.1$) to achieve NOx emissions below 100 ppmv when utilizing NH_3–H_2 mixtures effectively. Logically, this requires the use of a complementary secondary air injection to efficiently reduce unburned ammonia content. As for the $\%H_2$ content, its increase leads to a reduction of the NOx emissions due to limited N availability. From a practical viewpoint, the low sensitivity to V_{PSR}/V_{tot}, also demonstrated by the Sobol indices analysis, indicates that the CRN model is robust respect to this parameter, at least in the considered range of variation and for ammonia and hydrogen mixtures. Finally, an analysis is conducted to assess the effect of the kinetic mechanism on the estimation of NOx emissions. The results indicate that the values obtained using the Stagni et al. kinetic mechanism are in agreement with those obtained using the Gotama et al. kinetic mechanism. The CRN model developed here, together with the stochastic sensitivity analysis techniques, can be subsequently employed to identify and devise modifications of the combustor geometry as well as to evaluate the influence of additional operational parameters, including

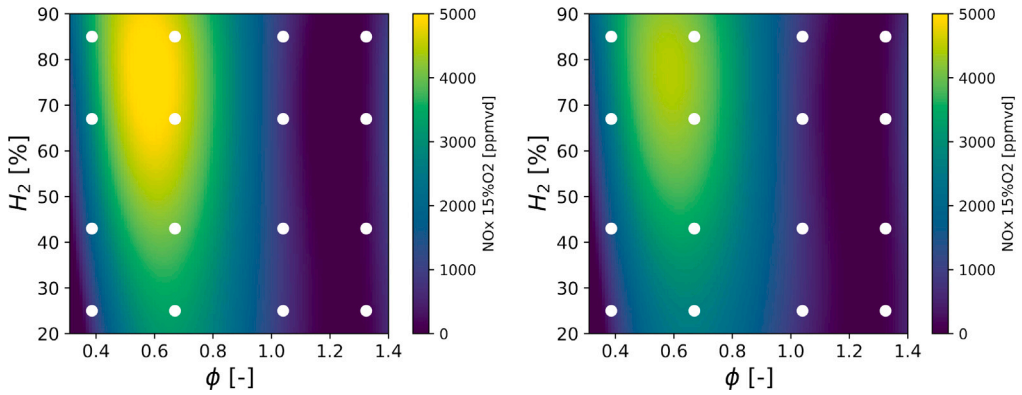

Fig. 10. Stochastic response surface of NOx emissions normalized to 15% O_2 in the flue gases in the parameter space of $\%H_2$ and ϕ with fixed reactor volume $V_{PSR}/V_{tot} = 20\%$ and inlet temperature $T_{in} = 430$ K for different kinetic mechanisms, (a) Gotama et al. [35] (b) Stagni et al. [34]. The white markers indicate quadrature points.

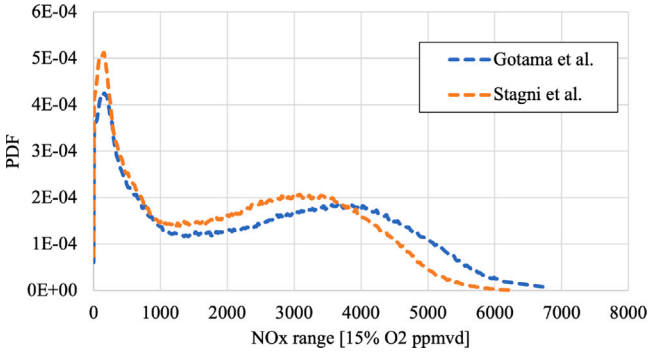

Fig. 11. Stochastic probability density function of NOx emissions using two kinetic mechanisms, i.e., Gotama et al. [35] (blue line) and Stagni et al. [34] (orange line).

pressure, on combustion efficiency and emissions. The outcomes could be then further investigated through detailed CFD simulations.

CRediT authorship contribution statement

Rachele Lamioni: Conceptualization, Data curation, Investigation, Methodology, Validation, Writing – original draft, Supervision. **Alessandro Mariotti:** Methodology, Writing – review & editing. **Maria Vittoria Salvetti:** Methodology, Writing – review & editing. **Chiara Galletti:** Conceptualization, Methodology, Writing – review & editing.

Declaration of competing interest

The authors declare that they have no known competing financial interests or personal relationships that could have appeared to influence the work reported in this paper.

Data availability

The data that has been used is confidential.

Acknowledgments

This research is funded by the Ministry of University and Research (MUR) as part of the PON 2014–2020 "Research and Innovation" resources - Green/Innovation Action - DM MUR 1062/2021. This work is supported by PNRR M4C2 - HPC, Big data and Quantum Computing (Simulazioni, calcolo e analisi dei dati e altre prestazioni - CN1) - CUP I53C22000690001 SPOKE 6 Multiscale modelling & Engineering applications and by the National Recovery and Resilience Plan (NRRP), Mission 4 Component 2 Investment 1.3 - Call for tender No. 1561 of 11.10.2022 of MUR - CUP B93C22001110006; funded by the European Union – NextGenerationEU, Project title "Network 4 Energy Sustainable Transition – NEST" with code PE0000021.

References

[1] D. Pugh, P. Bowen, A. Valera-Medina, A. Giles, J. Runyon, R. Marsh, Influence of steam addition and elevated ambient conditions on nox reduction in a staged premixed swirling NH_3/H_2 flame, Proc. Combust. Inst. 37 (4) (2019) 5401–5409, http://dx.doi.org/10.1016/j.proci.2018.07.091.

[2] A. Valera-Medina, M. Gutesa, H. Xiao, D. Pugh, A. Giles, B. Goktepe, R. Marsh, P. Bowen, Premixed ammonia/hydrogen swirl combustion under rich fuel conditions for gas turbines operation, Int. J. Hydrogen Energy 44 (16) (2019) 8615–8626, http://dx.doi.org/10.1016/j.ijhydene.2019.02.041.

[3] S. Wang, A.M. Elbaz, Z. Wang, W.L. Roberts, The effect of oxygen content on the turbulent flame speed of ammonia/oxygen/nitrogen expanding flames under elevated pressures, Combust. Flame 232 (2021) 111521, http://dx.doi.org/10.1016/j.combustflame.2021.111521.

[4] E.C. Okafor, Y. Naito, S. Colson, A. Ichikawa, T. Kudo, A. Hayakawa, H. Kobayashi, Experimental and numerical study of the laminar burning velocity of CH_4–NH_3–air premixed flames, Combust. Flame 187 (2018) 185–198, http://dx.doi.org/10.1016/j.combustflame.2017.09.002.

[5] H. Xiao, A. Valera-Medina, Chemical kinetic mechanism study on premixed combustion of ammonia/hydrogen fuels for gas turbine use, J. Eng. Gas Turb. Power 139 (8) (2017) http://dx.doi.org/10.1115/1.4035911.

[6] L. Mazzotta, F. D'Alessio, R. Meloni, S. Morris, B. Goktepe, R. Lamioni, M. Cerutti, C. Romano, C. Galletti, F. Creta, D. Borello, A. Valera-Medina, Modelling Ammonia-Hydrogen-Air Combustion and Emission Characteristics of a Generic Swirl Burner, in: Turbo Expo: Power for Land, Sea, and Air, Vol.2, 2023, V002T03A016, http://dx.doi.org/10.1115/GT2023-102803, Ceramics and Ceramic Composites; Coal, Biomass, Hydrogen, and Alternative Fuels.

[7] B. Mei, J. Zhang, X. Shi, Z. Xi, Y. Li, Enhancement of ammonia combustion with partial fuel cracking strategy: Laminar flame propagation and kinetic modeling investigation of $NH_3/H_2/N_2$/air mixtures up to 10 atm, Combust. Flame 231 (2021) 111472, http://dx.doi.org/10.1016/j.combustflame.2021.111472.

[8] S. Bragg, Application of Reaction Rate Theory To Combustion Chamber Analysis, Aeronautical Research Council London, 1953.

[9] A. Andreini, B. Facchini, Gas turbines design and off-design performance analysis with emissions evaluation, J. Eng. Gas Turb. Power 126 (1) (2004) 83–91, http://dx.doi.org/10.1115/1.1619427.

[10] S. Yousefian, G. Bourque, R.F. Monaghan, Uncertainty quantification of NOx and CO emissions in a swirl-stabilized burner, J. Eng. Gas Turb. Power 141 (10) (2019) 101014, http://dx.doi.org/10.1115/1.4044204.

[11] S. Yousefian, G. Bourque, R.F. Monaghan, Bayesian inference and uncertainty quantification for hydrogen-enriched and lean-premixed combustion systems, Int. J. Hydrogen Energy 46 (46) (2021) 23927–23942, http://dx.doi.org/10.1016/j.ijhydene.2021.04.153.

[12] M. Kanniche, Coupling CFD with chemical reactor network for advanced NOx prediction in gas turbine, Clean Technol. Environ. Policy 12 (2010) 661–670, http://dx.doi.org/10.1007/s10098-010-0293-5.

[13] D. Lee, J. Park, J. Jin, M. Lee, A simulation for prediction of nitrogen oxide emissions in lean premixed combustor, J. Mech. Sci. Technol. 25 (2011) 1871–1878, http://dx.doi.org/10.1007/s12206-011-0425-9.

[14] T.H. Nguyen, J. Park, C. Sin, S. Jung, S. Kim, Numerical investigation of the pressure effect on the NOx formation in a lean-premixed gas turbine combustor, Energy Fuels 35 (8) (2021) 6776–6784, http://dx.doi.org/10.1021/acs.energyfuels.0c02909.

[15] A. Colorado, V. McDonell, Emissions and stability performance of a low-swirl burner operated on simulated biogas fuels in a boiler environment, Appl. Therm. Eng. 130 (2018) 1507–1519, http://dx.doi.org/10.1016/j.applthermaleng.2017.11.047.
[16] Z. Saboohi, F. Ommi, M. Akbari, Multi-objective optimization approach toward conceptual design of gas turbine combustor, Appl. Therm. Eng. 148 (2019) 1210–1223, http://dx.doi.org/10.1016/j.applthermaleng.2018.11.082.
[17] R. Xue, C. Hu, V. Sethi, T. Nikolaidis, P. Pilidis, Effect of steam addition on gas turbine combustor design and performance, Appl. Therm. Eng. 104 (2016) 249–257, http://dx.doi.org/10.1016/j.applthermaleng.2016.05.019.
[18] S. Li, S. Zhang, H. Zhou, Z. Ren, Analysis of air-staged combustion of NH_3/CH_4 mixture with low NOx emission at gas turbine conditions in model combustors, Fuel 237 (2019) 50–59, http://dx.doi.org/10.1016/j.fuel.2018.09.131.
[19] S. Mashruk, H. Xiao, A. Valera-Medina, Rich-quench-lean model comparison for the clean use of humidified ammonia/hydrogen combustion systems, Int. J. Hydrogen Energy 46 (5) (2021) 4472–4484, http://dx.doi.org/10.1016/j.ijhydene.2020.10.204.
[20] D. Benedetto, S. Pasini, M. Falcitelli, C. La Marca, L. Tognotti, NOx emission prediction from 3-D complete modelling to reactor network analysis, Combust. Sci. Technol. 153 (1) (2000) 279–294, http://dx.doi.org/10.1080/00102200008947265.
[21] T. Faravelli, L. Bua, A. Frassoldati, A. Antifora, L. Tognotti, E. Ranzi, A new procedure for predicting NOx emissions from furnaces, Comput. Chem. Eng. 25 (4–6) (2001) 613–618, http://dx.doi.org/10.1016/S0098-1354(01)00641-X.
[22] M. Falcitelli, L. Tognotti, S. Pasini, An algorithm for extracting chemical reactor network models from CFD simulation of industrial combustion systems, Combust. Sci. Technol. 174 (11–12) (2002) 27–42, http://dx.doi.org/10.1080/713712951.
[23] M. Falcitelli, S. Pasini, N. Rossi, L. Tognotti, CFD+ reactor network analysis: an integrated methodology for the modeling and optimisation of industrial systems for energy saving and pollution reduction, Appl. Thermal Eng. 22 (8) (2002) 971–979, http://dx.doi.org/10.1016/S1359-4311(02)00014-5.
[24] A. Cuoci, A. Frassoldati, A. Stagni, T. Faravelli, E. Ranzi, G. Buzzi-Ferraris, Numerical modeling of NOx formation in turbulent flames using a kinetic post-processing technique, Energy Fuels 27 (2) (2013) 1104–1122, http://dx.doi.org/10.1021/ef3016987.
[25] A. Stagni, A. Cuoci, A. Frassoldati, T. Faravelli, E. Ranzi, A fully coupled, parallel approach for the post-processing of CFD data through reactor network analysis, Comput. Chem. Eng. 60 (2014) 197–212, http://dx.doi.org/10.1016/j.compchemeng.2013.09.002.
[26] R.F. Monaghan, R. Tahir, A. Cuoci, G. Bourque, M. Füri, R.L. Gordon, T. Faravelli, A. Frassoldati, H.J. Curran, Detailed multi-dimensional study of pollutant formation in a methane diffusion flame, Energy Fuels 26 (3) (2012) 1598–1611, http://dx.doi.org/10.1021/ef201853k.
[27] A.A. Perpignan, R. Sampat, A. Gangoli Rao, Modeling pollutant emissions of flameless combustion with a joint CFD and chemical reactor network approach, Front. Mech. Eng. 5 (2019) 63, http://dx.doi.org/10.3389/fmech.2019.00063.
[28] A. Kaluri, P. Malte, I. Novosselov, Real-time prediction of lean blowout using chemical reactor network, Fuel 234 (2018) 797–808, http://dx.doi.org/10.1016/j.fuel.2018.07.065.
[29] S. Gupta, P. Malte, S.L. Brunton, I. Novosselov, Prevention of lean flame blowout using a predictive chemical reactor network control, Fuel 236 (2019) 583–588, http://dx.doi.org/10.1016/j.fuel.2018.09.044.
[30] S. Chaturvedi, R. Santhosh, S. Mashruk, R. Yadav, A. Valera-Medina, Prediction of NOx emissions and pathways in premixed ammonia-hydrogen-air combustion using CFD-CRN methodology, J. Energy Inst. 111 (2023) 101406, http://dx.doi.org/10.1016/j.joei.2023.101406, URL https://www.sciencedirect.com/science/article/pii/S1743967123002350.
[31] D.G. Goodwin, H.K. Moffat, I. Schoegl, R.L. Speth, B.W. Weber, Cantera: An object-oriented software toolkit for chemical kinetics, thermodynamics, and transport processes, 2022, http://dx.doi.org/10.5281/zenodo.6387882, Version 2.6.0, https://www.cantera.org.
[32] J. Runyon, R. Marsh, P. Bowen, D. Pugh, A. Giles, S. Morris, Lean methane flame stability in a premixed generic swirl burner: Isothermal flow and atmospheric combustion characterization, Exp. Therm Fluid Sci. 92 (2018) 125–140, http://dx.doi.org/10.1016/j.expthermflusci.2017.11.019.
[33] A. Alnasif, S. Mashruk, M. Kovaleva, P. Wang, A. Valera-Medina, Experimental and numerical analyses of nitrogen oxides formation in a high ammonia-low hydrogen blend using a tangential swirl burner, Carbon Neutrality 1 (1) (2022) 24, http://dx.doi.org/10.1007/s43979-022-00021-9.
[34] A. Stagni, C. Cavallotti, S. Arunthanayothin, Y. Song, O. Herbinet, F. Battin-Leclerc, T. Faravelli, An experimental, theoretical and kinetic-modeling study of the gas-phase oxidation of ammonia, React. Chem. Eng. 5 (2020) 696–711, http://dx.doi.org/10.1039/c9re00429g.
[35] G.J. Gotama, A. Hayakawa, E.C. Okafor, R. Kanoshima, M. Hayashi, T. Kudo, H. Kobayashi, Measurement of the laminar burning velocity and kinetics study of the importance of the hydrogen recovery mechanism of ammonia/hydrogen/air premixed flames, Combust. Flame 236 (2022) 111753, http://dx.doi.org/10.1016/j.combustflame.2021.111753.
[36] J. Otomo, M. Koshi, T. Mitsumori, H. Iwasaki, K. Yamada, Chemical kinetic modeling of ammonia oxidation with improved reaction mechanism for ammonia/air and ammonia/hydrogen/air combustion, Int. J. Hydrogen Energy 43 (5) (2018) 3004–3014, http://dx.doi.org/10.1016/j.ijhydene.2017.12.066.
[37] D. Xiu, G.E. Karniadakis, The Wiener–askey polynomial chaos for stochastic differential equations, SIAM J. Sci. Comput. 24 (2) (2002) 619–644, http://dx.doi.org/10.1137/S1064827501387826.
[38] I.M. Sobol, Global sensitivity indices for nonlinear mathematical models and their Monte Carlo estimates, Math. Comput. Simul. 55 (1–3) (2001) 271–280, http://dx.doi.org/10.1016/S0378-4754(00)00270-6.
[39] D. Pugh, A. Valera-Medina, P. Bowen, A. Giles, B. Goktepe, J. Runyon, S. Morris, S. Hewlett, R. Marsh, Emissions performance of staged premixed and diffusion combustor concepts for an NH3/air flame with and without reactant humidification, J. Eng. Gas Turb. Power 143 (5) (2021) http://dx.doi.org/10.1115/1.4049451.
[40] Z. Li, S. Li, Kinetics modeling of NOx emissions characteristics of a NH3/H2 fueled gas turbine combustor, Int. J. Hydrogen Energy 46 (5) (2021) 4526–4537, http://dx.doi.org/10.1016/j.ijhydene.2020.11.024, URL https://www.sciencedirect.com/science/article/pii/S036031992034194X.